Differential expression of SUMO-specific protease 7 variants regulates epithelial–mesenchymal transition

Tasneem Bawa-Khalfe[a,1], Long-Sheng Lu[b], Yong Zuo[c], Chao Huang[b], Ruhee Dere[d], Feng-Ming Lin[b], and Edward T. H. Yeh[a,b,1]

[a]Department of Cardiology, University of Texas M. D. Anderson Cancer Center, Houston, TX 77030; [b]Texas Heart Institute/St. Luke's Episcopal Hospital, Houston, TX 77030; [c]Department of Biochemistry and Molecular Cell Biology, Shanghai Jiao Tong University School of Medicine, Shanghai 200025, China; and [d]Center for Translational Cancer Research, Institute of Biosciences and Technology, Texas A&M Health Cancer Center, Houston, TX 77030

Edited by Avram Hershko, Technion Israel Institute of Technology, Haifa, Israel, and approved September 6, 2012 (received for review June 4, 2012)

Two Sentrin/small ubiquitin-like modifier (SUMO)-specific protease 7 (SENP7) variants are naturally expressed in breast epithelia. Breast cancer (BCa) onset down-regulates the short SENP7 splice variant (SENP7S) and enhances the long transcript (SENP7L). Here, we show that SENP7L induction promotes gene expression profiles that favor aberrant proliferation and initiate epithelial–mesenchymal transition (EMT). SENP7L exhibits an interaction domain for the epigenetic remodeler heterochromatin protein 1 α (HP1α) and isopeptidase activity against SUMO-modified HP1α. Loss of this interaction domain, as observed with SENP7S, favors HP1α SUMOylation. SUMOylated HP1α is enriched at E2F-responsive and mesenchymal gene promoters, silences transcription of these genes, and promotes cellular senescence. Elevated SENP7L renders HP1α hypo-SUMOylated, which relieves transcriptional repression of the same genes and concurrently decreases transcription of epithelial-promoting genes via an HP1α-independent mechanism. Consequently, SENP7L levels correlate with EMT, motility, and invasiveness of BCa cells. Stable knockdown of elevated SENP7L levels lessens the dissemination of highly metastatic BCa cells to the lungs from primary implantation sites in in vivo studies. Thus, differential splicing of the *SENP7* regulates either tumor suppression or progression.

posttranslational-modification | epigenetics | dedifferentiation

Posttranslational modification by the small ubiquitin-like modifier (SUMO) family has garnered much attention in cancer biology. This could be attributed to the ability of SUMOylation to elicit a rapid and reversible change to a protein's function and/or subcellular localization. However, SUMOylation of one cellular target may be critical for normal cell physiology, whereas SUMO conjugation of another protein may promote aberrant growth. Hence, targeting the SUMO-conjugating machinery may be detrimental to cancer as well as normal cells.

Recently, the interest has shifted to the SUMO deconjugating enzymes or Sentrin/SUMO-specific proteases (SENP), which exhibit isopeptidase activity against a select subset of SUMOylated substrates. Although the expression of several SENPs is altered with onset of various carcinomas (1, 2), the physiological and/or pathophysiological function of many of the SENPs remains undefined. In addition, the six mammalian SENPs exhibit multiple splice variants that add to the functional diversity of the individual enzymes. SENP7 is an ideal example. Our laboratory used both extrinsic and experimental approaches to identify an *SENP7* gene transcript with an intact catalytic domain (3). Recent studies show that the catalytic domain of SENP7 exhibits activity against synthetic and endogenous SUMO-conjugated substrates (4–6). Although these studies demonstrate SENP7's deSUMOylating capabilities, there exists a paucity of literature on the biological function of SENP7. In the present article we characterize two *SENP7* transcript variants whose dueling functions support either tumor suppressive or potentiating pathways. To initiate a specific pathway, the SENP7 isoforms modulate differential epigenetic profiles in cancer cells.

The chromobox (CBX) homolog superfamily consists of well-characterized epigenetic remodeling proteins. Recently we demonstrated that SENP2-mediated deSUMOylation is critical for directing the function of CBX4/Pc2 in development (7). SUMOylation of other CBX proteins, specifically the heterochromatin protein 1 (HP1) isoforms, regulates their heterochromatic localization and subsequent gene silencing functions that maintain normal cell biology (8, 9). Clearly SUMO modification regulates the function of CBX proteins; however, it is unknown how SUMOylation of CBX proteins contributes to the epigenetic reprogramming of cancer cells. In cancer biology, CBX5/HP1α dictates the invasive nature of breast cancer (BCa) cells (10). Expression of HP1α, unlike the other isoforms, correlates with BCa onset and enhanced diagnosis of cancer metastasis (11, 12). To acquire invasive properties and initiate the metastatic cascade, cancer cells repress epithelial genes and elicit de novo transcription of mesenchymal genes to promote epithelial–mesenchymal transition (EMT) (13). Although previous studies suggest that HP1α directs BCa invasiveness, the ability of HP1α to establish gene profiles that favor EMT has not been investigated. The present study demonstrates that SENP7 variants dictate the level of HP1α SUMOylation, which in turn contributes to epigenetic reprogramming for EMT.

Results

Since our initial report (3), two *SENP7* transcript variants have been validated in the RefSeq database (Fig. 1*A*); the full-length SENP7 mRNA (SENP7L, accession no. NM_020654.3) and a shorter exon 6-deficient variant (SENP7S, accession no. NM_001077203.1). SENP7L and SENP7S are expressed differently in normal human breast epithelia, with tissue from independent patient samples exhibiting substantially greater mRNA of splice variant SENP7S than of SENP7L (Fig. 1*B*). Expression of SENP7L in breast epithelia is comparable to levels found in other tissues (Fig. S1*A*). As opposed to all *SENP7* transcripts (Fig. S1*B*), the SENP7L message increases with the onset of nonmetastatic BCa in human patient samples ($P < 0.05$; Fig. 1*C*). Tumor metastasis further potentiates SENP7L mRNA levels in the primary tumor samples ($P = 0.05$ vs. nonmetastatic carcinoma samples; Fig. 1*C*) and prompts SENP7L to become the major *SENP7* transcript (Fig. S1 *C* and *D*). In contrast, SENP7S is reduced in BCa patients (either non- or metastatic carcinoma vs. normal, $P < 0.05$; Fig. 1*D*). A similar trend is observed at a cellular level with elevated SENP7L mRNA in

Author contributions: T.B.-K. designed research; T.B.-K., L.-S.L., Y.Z., C.H., R.D., and F.-M.L. performed research; T.B.-K., L.-S.L., Y.Z., C.H., R.D., F.-M.L., and E.T.H.Y. analyzed data; and T.B.-K. and E.T.H.Y. wrote the paper.

The authors declare no conflict of interest.

This article is a PNAS Direct Submission.

[1]To whom correspondence may be addressed. E-mail: tbawa@mdanderson.org or etyeh@mdanderson.org.

This article contains supporting information online at www.pnas.org/lookup/suppl/doi:10.1073/pnas.1209378109/-/DCSupplemental.

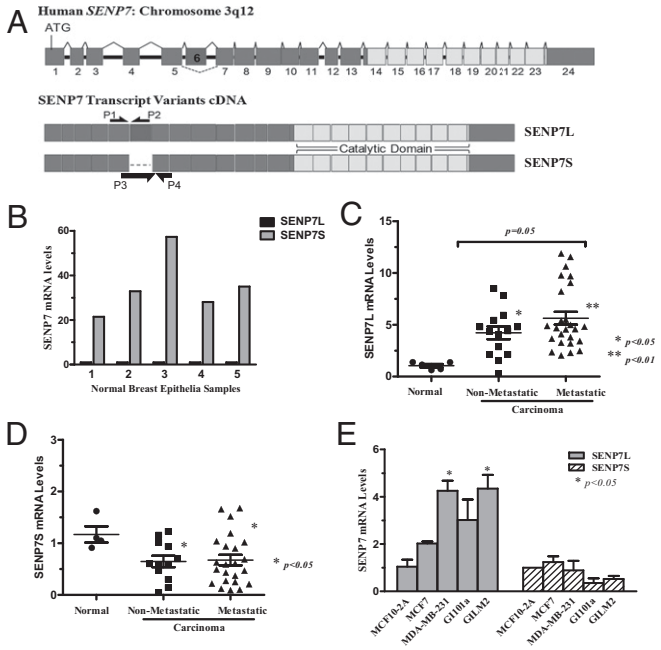

Fig. 1. Inverse expression of two SENP7 transcripts with onset of BCa. (*A*) Schematic illustrating the alternative exon 6 splicing (dashed lines below) from the human *SENP7* to generate two transcript variants (SENP7L and SENP7S). SENP7L and SENP7S mRNA levels were assessed using specific primers (P1/P2 and P3/P4, respectively) for the highlighted regions. (*B*) Five normal human mammary epithelia samples independently exhibit higher SENP7S than SENP7L message. Data represent the fold change in SENP7S compared with SENP7L mRNA levels. (*C*) An induction of SENP7L mRNA occurs with nonmetastatic and metastatic carcinoma compared with normal tissue (ANOVA and Dunnett's, $P < 0.05$ and $P < 0.001$, respectively, $n = 48$). SENP7L mRNA levels are greater in patients with metastatic than nonmetastatic disease (Student *t* test, $P = 0.05$). (*D*) The same samples exhibit lower SENP7S mRNA with carcinoma (vs. normal tissue, ANOVA and Dunnett's, $P < 0.05$). (*E*) Highly metastatic BCa cell lines MDA-MB-231, GI101a, and GILM2 express higher SENP7L than SENP7S ($n = 2$–3). Data in *C*–*E* represent the fold change of the indicated transcript in cancer tissue or cells compared with normal tissue or MCF710-2A cells.

highly metastatic human BCa cell lines (MDA-MB-231, GI101a, GILM2) compared with normal MCF10-2A (Fig. 1*E*). Collectively, the data indicate that SENP7S is the dominant in normal breast tissue, whereas SENP7L is elevated in aggressive carcinomas. Hence, we sought to determine whether the increase in the SENP7L variant could play a role in BCa pathogenesis.

Yeast two-hybrid analysis suggested association between SENP7L and HP1α, and subsequent immunoprecipitation confirmed that SENP7L, but not SENP7S, binds HP1α (Fig. S1*E*). This interaction does not require catalytic activity: both the active wild-type SENP7L and the catalytically inactive mutant (SENP7Lm) bind endogenous HP1α efficiently (Fig. S1*F*). To identify the HP1α-interaction domain on *SENP7* transcripts, we first targeted the PRVIL sequence as a canonical PXVXL motif (described in *SI Materials and Methods*). This pentapeptide sequence is located on exon 6 of *SENP7* and consequently present on the SENP7L but not SENP7S. PRVIL is conserved among mammals because it appears on the N terminus of multiple full-length *SENP7* orthologs (Fig. 2*A*). When alanine replaces P, V, and L, SENP7L interaction with HP1α is lost; hence, SENP7L binds HP1α via a PXVXL motif (Fig. 2*B*). The other five SENPs do not exhibit an analogous PRVIL sequence.

Chromatin-bound HP1α is modified by endogenous SUMO2/3 but not SUMO1 with SENP7 reduction (Fig. 2*C*); targeted siRNA and shRNA independently decrease SENP7 mRNA in multiple human BCa cells (Fig. S2 *A* and *B*, respectively). In contrast, all three SUMO isoforms conjugate HP1α in in vitro conditions (Fig. 2*D* and Fig. S3*A*). SUMO2/3-conjugated HP1α is readily observed in human BCa cells with less SENP7L transcript (MCF10-2A compared with GI101a or GILM2; Fig. S3*B*), indicating an inverse correlation between HP1α SUMOylation and SENP7L expression. Hence, we wanted to assess whether SENP7L deSUMOylates HP1α more efficiently than the HP1α interaction-deficient SENP7L mutant (PXVXLdf). Maximum SUMOylation of endogenous HP1α was maintained with overexpression of SUMO2 and the E3 ligase PIAS4 (lane 1 and 2, Fig. 2*D*). SENP7L induction decreases SUMOylated HP1α levels (lane 3, Fig. 2*D*, and lane 4, Fig. S3*C*), whereas inactive SENP7Lm does not (lane 4, Fig. 2*D*). Similar to SENP7S (Fig. S3*C*), the PXVXLdf mutant (Fig. 2*B*) also cannot deSUMOylate modified HP1α (lane 5, Fig. 2*D*). Hence, the data suggest that an intact catalytic domain and PXVXL sequence is required for SENP7L to deSUMOylate HP1α.

When SUMO2 is elevated, the wild-type HP1α (HP1α-WT) is recruited to trimethylated histone 3 K9 (H3K9m3) in MDA-MB-231 cells (Fig. 3 *A* and *B*). To validate the importance of SUMOylation in directing HP1α's subnuclear localization, a SUMO-deficient HP1α mutant (K32R) was generated (Fig. S3*D*). Unlike HP1α-WT, K32R does not readily bind the silenced chromatin mark H3K9m3 (Fig. S3*E*), even under hyper-SUMOylation conditions (Fig. 3 *C* and *D*). Therefore, unlike mutation of individual K residues in the HP1α hinge region, which causes

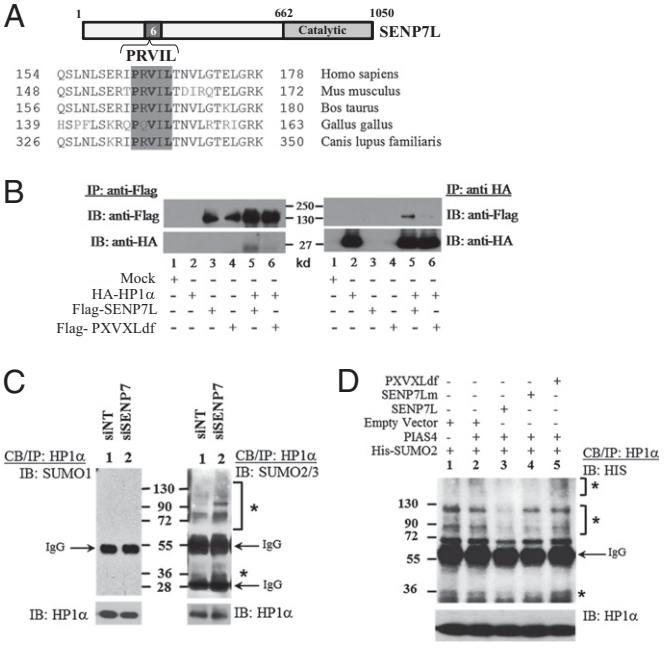

Fig. 2. SENP7L transcript interacts with chromatin-associated HP1α and dictates the level of SUMO2/3-modified HP1α. (*A*) Schematic representation of the HP1α interaction motif (PRVIL) on the human SENP7L with respect to exon 6 and the catalytic domain. Alignment of the human SENP7L with other mammalian full-length SENP7 orthologs indicates conservation of the PXVXL sequence. (*B*) The interaction of Flag-tagged SENP7L and HA-HP1α was confirmed with independent pull-down experiments in COS cells. HP1α interaction is lost with mutation of the PRVIL sequence to ARAIA on the SENP7L. (*C*) After siSENP7 knockdown for 48 h, endogenous SUMO2/3 modification of chromatin-bound HP1α was observed in MCF7 cells. (*D*) SUMOylation of endogenous HP1α is modestly potentiated with PIAS4 (lane 2) in MCF7 cells. SUMO-modified HP1α is reduced by SENP7L (lane 3) but not inactive SENP7Lm (lane 4) or HP1α interaction-deficient PXVXLdf (lane 5). Asterisks highlight SUMO-conjugates in *C* and *D*.

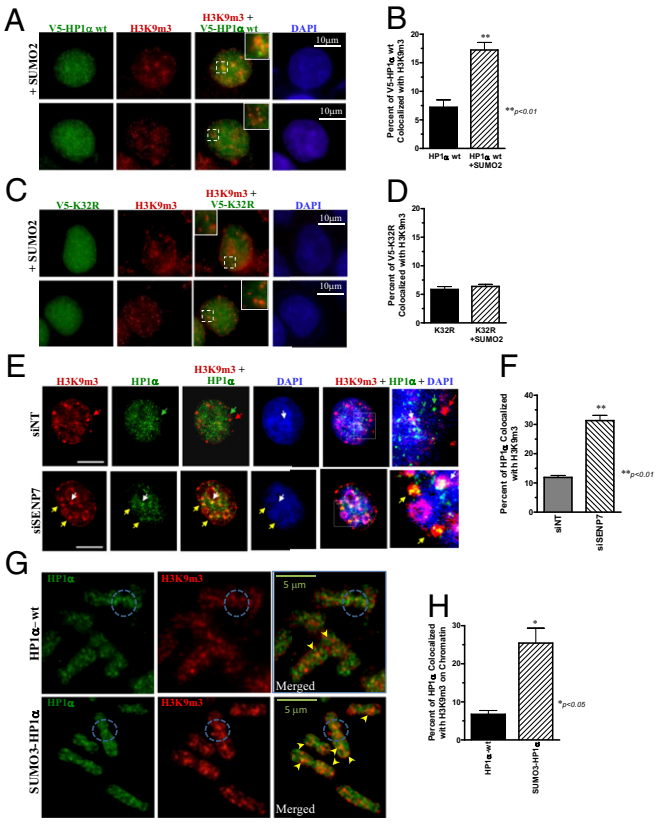

Fig. 3. SUMOylation regulates HP1α chromatin localization. (*A*) The V5-tagged HP1α-WT more readily colocalizes with H3K9m3 in the presence of SUMO2 for 48 h in MDA-MB-231 cells. (*B*) Graph shows that SUMO2 overexpression increases HP1α-H3K9m3 interaction in multiple MDA-MB-231 cells (n = 8–9, Student t test, $P < 0.01$). (*C* and *D*) Hyper-SUMO conditions do not alter V5-K32R-H3K9m3 association in the same cell line (n = 6–7). (*E* and *F*) Endogenous HP1α colocalizes with H3K9m3 more efficiently after siSENP7, but not siNT, treatment in MCF7 cells (n = 8–9, Student's test, $P < 0.01$). This interaction occurs inside (white arrow) and outside (yellow arrow) highly condensed chromatin, which is highlighted by intense DAPI staining. (*G* and *H*) SUMO3-HP1α binds H3K9m3-rich loci throughout the chromosome (yellow arrowhead) and near the centromere (highlighted with a circle) more efficiently than HP1α-WT.

residual SUMOylation at alternative sites (8), the SUMOylation of K32 within the chromodomain of HP1α seems to be unique in that it is critical for HP1α to bind H3K9m3. Hence, the K32 site is similar to the SUMO acceptor site on the chromodomain of the fission yeast HP1 homolog Swi6, which prevents localization to heterochromatic regions when deleted (9).

Endogenous HP1α is defused throughout the nucleus and binds H3K9m3 primarily in condensed chromatin regions, which are heavily DAPI-stained (white arrow on final panel, Fig. 3*E*), in nontargeting siRNA (siNT)-treated MCF7 cells. However, SENP7 knockdown concentrates HP1α's distribution (Fig. 3*E* and Fig. S4*A*) and enhances HP1α-H3K9m3 association (Fig. 3 *E* and *F*). This interaction occurs both within (white arrow, Fig. 3*E*) and outside (yellow arrows, Fig. 3*E*) condensed chromatin regions. SUMO3-fused HP1α (SUMO3-HP1α) constructs also appear in similar concentrated loci but under native conditions (Fig. S4 *B* and *C*). Whereas HP1α-WT is present on the chromosome in a speckled pattern, SUMO3-HP1α is uniformly distributed at H3K9m3 loci throughout both chromosome arms (yellow arrowheads, Fig. 3*G*) and at the pericentric region (highlighted circle, Fig. 3*G*). Hence, SUMO3-HP1α more efficiently binds H3K9m3-rich domains than HP1α-WT (Fig. 3*H*).

To see whether SUMOylation affects HP1α's recruitment to specific gene loci, we conducted a series of ChIP experiments that evaluated HP1α's localization at the promoter of previously identified HP1α-target genes (14–16). SENP7-targeted siRNA (siSENP7) enriches HP1α at the promoter of proliferation-regulating E2F-response genes *dihydrofolate reductase* (*DHFR*), *thymidylate synthase* (*TS*), and *CDC25a* (Fig. 4*A*). Although HP1α is present at the E2F-unresponsive *c-fos* promoter under native conditions, reducing SENP7 does not increase HP1α levels at the *c-fos* promoter (Fig. 4*A*). Therefore, the data suggest that SENP7 loss prompts HP1α's enrichment selectively at E2F-responsive gene promoters.

Because HP1α modulates BCa cell invasiveness (10), we assessed HP1α's presence at the promoter of the invasion-regulating *vimentin* under normal and reduced SENP7 conditions. HP1α binds the *vimentin* promoter at detectable levels in siNT-treated MCF7 cells (Fig. 4*A*), whereas SENP7 loss elevates the recruitment of HP1α to this mesenchymal gene promoter (Fig. 4*A*). In contrast,

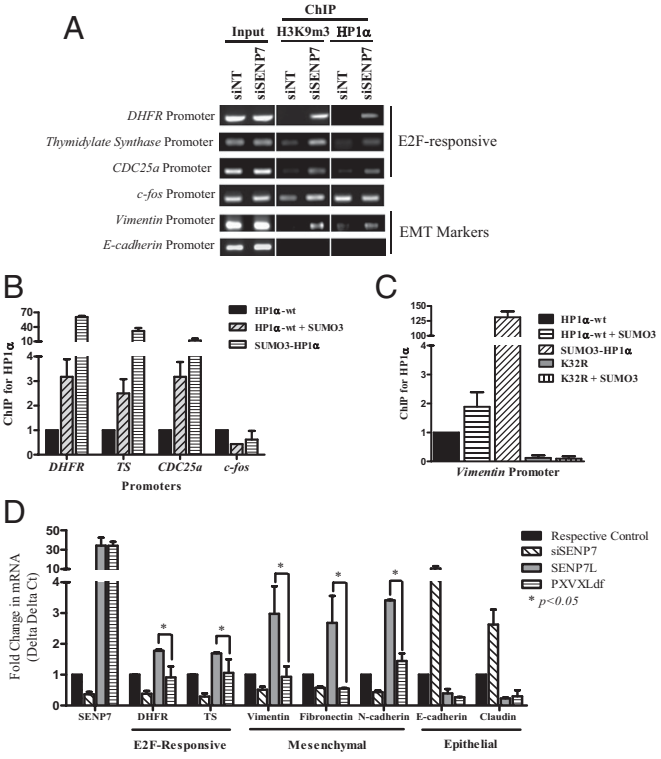

Fig. 4. SENP7L and concomitantly SUMOylation define HP1α's recruitment to specific gene promoters and gene silencing function. (*A*) ChIP with either H3K9m3 or HP1α antibody was followed by RT-PCR (representative of three independent experiments). Knockdown with siSENP7 but not siNT in MCF7 cells for 48 h enhances HP1α recruitment at E2F-regulated gene and *Vimentin* promoters; it also induces H3K9m3 at the same promoters. (*B*) Real-time PCR of ChIP samples (n = 3) indicates that SUMO3 overexpression enriches HP1α-WT at E2F-responsive gene promoters (*DHFR*, *TS*, and *cdc25a*) but not the E2F-unresponsive *c-fos* promoter in MDA-MB-231 cells; the SUMO3-HP1α construct exhibits a similar distribution pattern. (*C*) SUMO3-HP1α's presence is substantially greater than HP1α-WT at the *Vimentin* promoter as observed in independent ChIP experiments (n = 3). K32R mutants do not bind the *Vimentin* promoter, and no change occurs with SUMO3 overexpression in MDA-MB-231 cells. (*D*) Real-time PCR analysis of MCF7 cells indicates that SENP7, compared with NT, siRNA treatment lowers E2F-responsive and mesenchymal mRNA but increases the mRNA of epithelial markers. SENP7L overexpression elevates E2F-responsive and mesenchymal mRNA compared with EV. Student t test suggest a significant difference between SENP7L and PXVXLdf mutant (n = 5, $P \leq 0.05$).

HP1α does not bind the epithelial-inducing *E-cadherin (E-cad)* promoter after either siNT or siSENP7 treatment.

SUMO3 overexpression in MDA-MB-231 cells produces a similar HP1α recruitment to E2F-responsive genes and *vimentin* (Fig. 4 *B* and *C*, respectively), but not *c-fos*, promoters (Fig. 4*B*). SUMO3-HP1α exhibits an even greater affinity for these same promoters than HP1α-WT (Fig. 4 *B* and *C*). Whereas HP1α-WT binds the *vimentin* promoter under native conditions, K32R does not (Fig. 4*C*). Even hyper-SUMOylation conditions cannot force K32R to *vimentin* (Fig. 4*C*) or E2F-regulated gene promoter (Fig. S4*D*), suggesting that this SUMO acceptor site is required for HP1α's recruitment to specific promoters.

Interestingly, HP1α's enrichment at E2F-responsive and *vimentin* gene promoters occurs concurrently with enhanced H3K9m3 near these same promoters (Fig. 4*A*). Induction of this silenced chromatin mark at the promoter loci suggests transcriptional repression of these genes with SENP7 knockdown. This is indeed the case: mRNA levels of DHFR, TS, vimentin, and two additional mesenchymal markers (fibronectin and *N*-cadherin) are reduced after siSENP7 in MCF7 cells (Fig. 4*D*). The same mRNAs are reduced with expression of SUMO3-HP1α in MDA-MB-231 cells (Fig. S4*E*).

Conversely, maintaining hypo-SUMOylated HP1α with overexpression of SENP7L (Fig. 2*E*) elevates the mRNA of E2F-responsive and mesenchymal genes (Fig. 4*D*). In contrast, increasing PXVXLdf exhibits lower DHFR, TS, vimentin, fibronectin, and *N*-cadherin mRNA levels than SENP7L ($P < 0.05$, Student *t* test; Fig. 4*D*) but comparable to empty vector (EV) control. Although elevated after siSENP7, the mRNA of epithelial markers E-cad and claudin is repressed by overexpression of either SENP7L WT or PXVXLdf mutant (Fig. 4*D*). SENP7 reduction also enhances E-cad mRNA in MDA-MB-231 cells, but SUMO3-HP1α does not alter E-cad mRNA (Fig. S4*E*). Hence, it seems that SENP7L modulates the mRNA levels of epithelial-promoting genes via an HP1α-independent mechanism.

Interestingly, long-term (120 h) SENP7 knockdown causes enlarged flattened cells with intracellular vacuoles (Fig. S5*A*), reminiscent of senescence cell morphology. SENP7 loss causes additional hallmark signs of senescent cells; specifically, siSENP7-treated cells exhibit β-gal staining (Fig. 5 *A* and *B*), senescence-associated heterochromatin foci as indicated by concentrated DAPI and H3K9m3 staining (Fig. 5 *C* and *D*), decreased cell growth (Fig. S5*B*), and MNase-insensitive condensed chromatin (Fig. S5*C*).

Transient SENP7L overexpression (48 h) causes MCF7 cells to become irregular in shape and more loosely dispersed than the tightly clustered cells transfected with either EV or SENP7Lm (Fig. 5*E*). Cells with elevated SENP7L instead resemble TGF-β–treated MCF7 cells (Fig. 5 *E* and *F*). Previous studies have demonstrated that TGF-β treatment causes EMT with transcriptional repression of epithelial-promoting genes, including *E-cad*, and activation of mesenchymal-inducing genes like *vimentin* (17, 18). Hence E-cad and vimentin expression was evaluated in MCF7 cells treated with TGF-β, or transfected with either EV or SENP7L. Consistent with mRNA data (Fig. 4*D*), elevated SENP7L levels caused a loss of E-cad equivalent to TGF-β treatment and prompted vimentin expression unlike EV (Fig. 5*G*).

Consistent with the EMT morphology (Fig. 5*G*), overexpression of SENP7L, but not PXVXLdf (Fig. S6*A*), enhances motility of MCF7 control clones shNT-MCF7 (Fig. 6*A*). To further determine whether the SENP7L transcript solely contributes to the mesenchymal nature of cancer cells, we evaluated BCa cell motility after knockdown of all catalytically active SENP7 transcripts. Stable or transient SENP7 reduction significantly decreases the migratory property of MCF7 and two additional BCa cells (Fig. 6*A* and Fig. S6*B*). Overexpression of SENP7L completely rescues the reduced motility of stable MCF7 clones with lower SENP7 levels (shSP7-MCF7, Fig. 6*A*). In contrast, neither SENP7S nor the

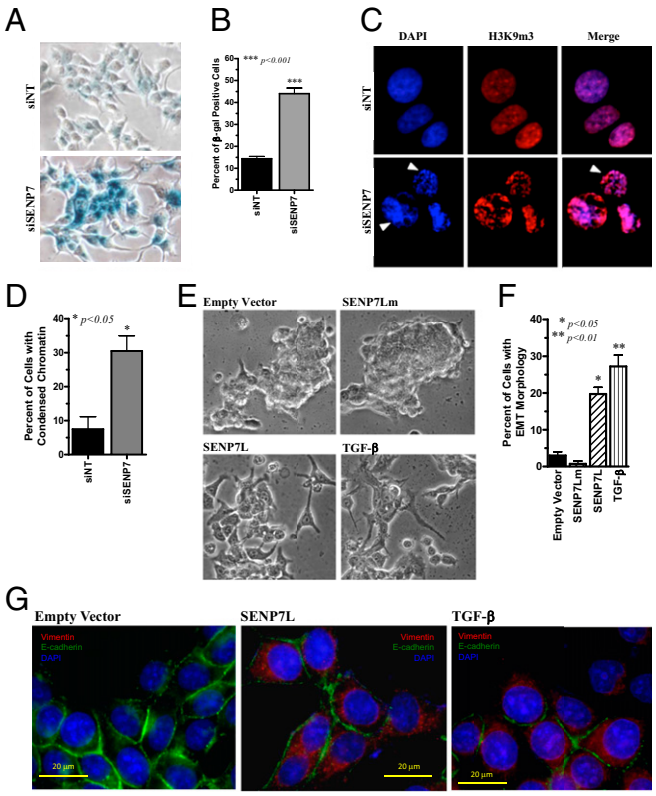

Fig. 5. SENP7L regulates cellular senescence and EMT. Exposure of MCF7 cells to SENP7 siRNA for 120 h increases β-galactosidase uptake (*A* and *B*) and condensed chromatin as observed with DAPI and H3K9m3 staining (*C* and *D*). (*E* and *F*) Both transient (48 h) SENP7L and TGF-β (10 ng/mL) treatments produced more dispersed, stellated MCF7 cells (defined as EMT morphology) compared with EV (ANOVA and Tukey's, $P < 0.05$ and $P < 0.01$, respectively); SENP7L mutant transfection had no effect. (*G*) Immunofluorescence evaluation indicated reduced E-cad and simultaneous increased Vimentin after both treatments compared with EV treatment. Each image is representative of three to four independent experiments.

PXVXLdf altered the shSP7-MCF7 migration (Fig. S6*C* and Fig. 6*A*, respectively). Because SENP7L-HP1α interaction is important for BCa cell motility, we assessed how changes to HP1α SUMOylation affect motility. MCF7 clones treated with HP1α-targeted siRNA (siHP1α) exhibited massive amounts of cell death. Consequently, to ensure adequate HP1α levels for cell survival, siHP1α was combined with transfection of either HP1α-WT or K32R (Fig. S6*D*). When supplemented with HP1α-WT, shSP7-MCF7 clones are less motile than shNT-MCF7 (Fig. 6*B*) and resemble EV-transfected shSP7-MCF7 (Fig. 6*A*). Although K32R expression enhances shSP7-MCF7 motility, the migratory property of these cells is less than HP1α-WT–expressing shNT-MCF7 clones (Fig. 6*B*).

Similarly, reducing all catalytically active SENP7 isoforms prompts a reduction in GILM2 cells' invasiveness (Fig. 6*C*). Diminished GILM2-shSENP7 invasiveness is completely reverted with SENP7L expression (Fig. 6*C*), suggesting that SENP7L is the sole transcript required for the invasive and migratory (Fig. 6*A*) property of BCa cells. Consequently, we postulated that decreasing the large SENP7L population present natively in GILM2 cells (Fig. 1*E*) should affect the tumorigenic and metastatic potential of these aggressive BCa cells. When injected into the mammary fat pad of nude mice with their respective controls, GILM2-shSENP7 cells produce smaller primary tumors in xenografts compared with GILM2-shNT control cells ($P < 0.05$, Student *t* test; Fig. 6*D*). Similar results are obtained in GI101a

CELL BIOLOGY

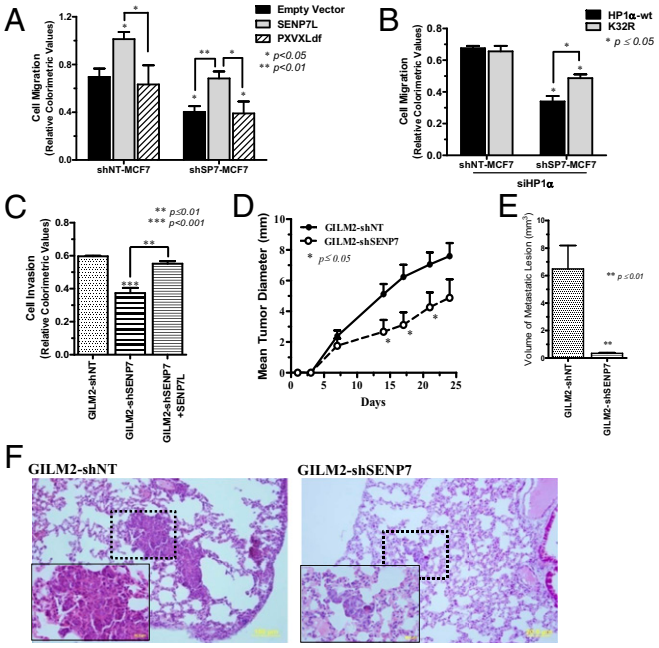

Fig. 6. Induction of SENP7L contributes to the tumorigenic property of BCa cells. (*A*) Stable shRNA-expressing MCF7 clones were transiently transfected with the indicated plasmid. EV-transfected shNT-MCF7 clones are significantly different from SENP7L-transfected shNT-MCF7, EV-transfected shSP7-MCF7, and PXVXLdf-transfected shSP7-MCF7 clones (ANOVA and Dunnett's, $P < 0.05$). Brackets indicate Student *t* test results for comparison of specific treatment groups. Data represent mean ± SEM from three to four independent experiments. (*B*) Endogenous HP1α was down-regulated with HP1α-targeting siRNA and simultaneously replaced by transfection of either HP1α-WT or K32R. The shSP7-MCF7 cells with either WT or K32R are less motile than shNT-MCF7 cells with HP1α-WT (ANOVA and Dunnett's, $P < 0.05$, $n = 3$), but K32R does slightly enhance shSP7-MCF7 motility compared with HP1α-WT expression (Student *t* test, $P \leq 0.05$). (*C*) Invasion through extracellular matrix is decreased in stable GILM2-shSENP7 ($n = 3$, Student *t* test, $P < 0.001$); this is reverted with SENP7L overexpression. (*D*) GILM2-shSENP7 ($n = 10$) produced dramatically smaller tumors in the mammary fat pad of female nude mice than control GILM2-shNT ($n = 6$, Student *t* test, $P \leq 0.01$). (*E* and *F*) GILM2-shNT cells ($n = 9$) formed larger metastatic lesions in the lung (Student *t* test, $P < 0.01$) than GILM2-shSENP7 ($n = 5$). An average metastatic niche in lung tissue from the indicated xenograft is shown.

cells ($P \leq 0.01$, Student *t* test; Fig. S6*D*). Gene expression analysis indicates lower mRNA of E2F-responsive genes and *vimentin* in tumor mass from GI101a-shSENP7 and GILM2-shSENP7 than their respective shNT control xenografts (Fig. S6*F*), similar to results from cultured cells (Fig. 4*D*).

Four weeks after removal of 12-mm-diameter primary tumors, lung tissue harvested from GILM2-shNT exhibited a greater number ($n = 11$) of metastatic lesions than GILM2-shSENP7 ($n = 5$) xenografts. The metastatic foci were also smaller in GILM2-shSENP7 thanin GILM2-NT xenografts ($P < 0.01$, Student *t* test; Fig. 6 *E* and *F*). Hence, the elevated SENP7L found in GILM2 cells are critical for its metastatic capability.

Discussion

Two *SENP7* transcripts exhibit inverse expression and function in breast cells. The shorter splice variant, SENP7S, is highly expressed in normal breast cells (Fig. 1*B*), whereas SENP7L is augmented in BCa cells (Fig. 1 *C* and *E* and Fig. S1*C*). Fluctuation of specific variants is a common event that contributes to the complexity of the cancer environment. SENP7L induction and concomitant SENP7S loss could occur via multiple mechanisms. First, the *SENP7* sequence could undergo mutations that prevent recognition of splice sites that facilitate generation of SENP7S. Second, BCa onset may causes changes in the splicing machinery, specifically reduction of splicing enhancers and induction of splicing silencers. Exactly which mechanism contributes to SENP7L enhancement is beyond the scope of this article but needs to be investigated further.

Clearly maintaining elevated SENP7L levels is beneficial for cancer cells because SENP7L orchestrates three events: (*i*) overcoming the growth barriers, (*ii*) de novo mesenchymal gene expression, and (*iii*) repressing transcription of epithelial genes. The first two events are dependent on HP1α deSUMOylation.

The PXVXL sequence of SENP7L is required for interaction with HP1α and deSUMOylation of HP1α in human BCa cells (Fig. 2 *B* and *D*). As we were preparing this report, a brief communication also reported an interaction between SENP7 and HP1α in mouse fibroblast cells but did not identify the PXVXL motif or its significance to HP1α SUMOylation (6). The authors did demonstrate that reducing SENP7 levels in these fibroblast cells decreases HP1α's recruitment to the H3K9m3-rich pericentric region (6). In contrast, HP1α-H3K9m3 association is enhanced with reduction of SENP7 (Fig. 3*F*) or under hyper-SUMOylation conditions (Fig. 3*B*) in human BCa cells. Consistently, SUMO3-HP1α constructs are readily localized with H3K9m3 at and outside the pericentric region (Fig. 3 *G* and *H*). The difference between the previous results and our present findings could be due to the different species of cells, the SUMO isoform conjugated to HP1α, or different regulatory mechanisms that persist with HP1α-SENP7 interaction in normal vs. cancer cells. It is also intriguing to speculate that an additional uncharacterized *SENP7* transcript may be present in the mouse fibroblast, but not human BCa, cells.

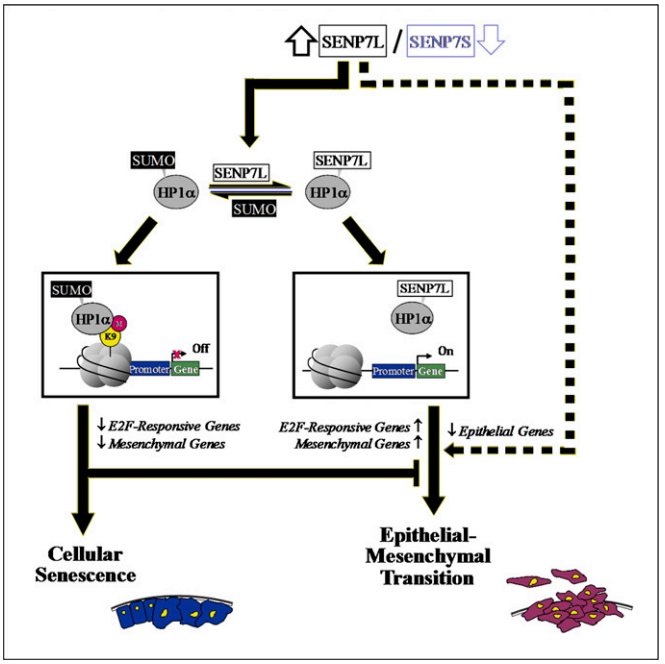

Fig. 7. SENP7L levels dictate BCa cells' choice between senescence and EMT. Onset of cancer in breast epithelia decreases the SENP7S splice variant and increases SENP7L, which expresses an HP1α-interaction motif. Loss of SENP7L-HP1α interaction causes HP1α hyper-SUMOylation, an enrichment of HP1α at E2F-responsive and mesenchymal gene promoters, silences transcription of these genes, and elicits cellular senescence. Induction of SENP7L maintains hypo-SUMOylated HP1α, which relieves HP1α-mediated repression of proliferation-promoting E2F-responsive genes as well as mesenchymal genes. SENP7L decreases epithelial gene expression via an unidentified HP1α-independent pathway (dashed line), and concurrently with the HP1α-dependent pathway promotes dedifferentiation.

In human BCa cells, SUMO modification also directs HP1α to specific promoter loci (Fig. 4). When present at E2F-reponsive gene promoters, HP1α enhances the recruitment of other chromatin regulators, including histone methyltransferases, and potentiates H3K9m3 to silence E2F-responsive genes (14–16, 19). The present data show that HP1α SUMOylation enriches it at E2F-responsive gene promoters (Fig. 4 *A* and *B*) and represses transcription of these genes (Fig. 4*D* and Fig. S4*E*). Silencing E2F-responsive genes causes cellular senescence irrespective of upstream mediators like p53 and Rb (14, 20). Therefore, because SENP7 knockdown suppresses E2F-responsive gene transcription (Fig. 4*D*), it is not surprising that SENP7 loss causes cellular senescence in BCa cells (Fig. 5 *A–D*).

Recent studies suggested that senescence of cancer cells is modulated by transcription factors that initiate EMT; loss of these transcription factors prevents EMT and elicits cellular senescence (21, 22). The mechanism for simultaneous regulation of both processes was presented as "collateral damage" and hence remains poorly defined. Like these transcription factors, chromatin-remodeling proteins are also capable of facilitating the EMT response (23, 24). In the present study we demonstrate that the interaction of SENP7L with HP1α and consequently HP1α's SUMOylation state dictates both cellular senescence and de novo mesenchymal gene transcription in BCa cells. SENP7 knockdown enhances HP1α's enrichment at the *vimentin* promoter and reduces vimentin and additional mesenchymal transcripts (Fig. 4 A, *C*, and *D*). Conversely, MCF7 cells, which are epithelium-like, exhibit de novo transcription of vimentin and several mesenchymal genes with transient overexpression of SENP7L, but not the HP1α interaction-deficient SENP7L mutant (Fig. 4*D*).

SENP7L also dictates transcription of two epithelial genes, *E-cad* and *claudin*, but independent of HP1α. First, although SENP7 directs HP1α to several promoters, HP1α is not observed at the *E-cad* promoter (Fig. 4*A*). Second, overexpression of either SENP7L or PXVXLdf produces an equivalent E-cad/claudin mRNA loss (Fig. 4*D*), suggesting that the HP1α motif is dispensable for SENP7L's regulation of epithelial genes. The pathway for this regulation is currently unknown.

SENP7L induction elicits dedifferentiation of BCa cells to support a more mesenchymal cell morphology (Fig. 5 *E–G*). Consistently, SENP7L potentiates the migratory properties of stagnant MCF7 control clones while restoring the reduced motility of shSP7-MCF7 clones (Fig. 6*A*). Unlike SENP7L, PXVXLdf cannot (*i*) elicit de novo mesenchymal gene transcription (Fig. 4*D*) or (*ii*) alter the migratory potential of either control or shSP7-MCF7 clones (Fig. 6*A*). Similarly, maintaining a large pool of hypo-SUMOylated HP1α (K32R) only partially, whereas SENP7L overexpression completely, rescues the reduced shSP7-MCF7 cells motility (Fig. 6 *B* and *A*, respectively). This is because SENP7L, unlike PXVXLdf or K32R, affects both "arms" of the EMT process: (*i*) mesenchymal gene transcription dependent on HP1α deSUMOylation, and (*ii*) inhibiting epithelial gene transcription independent of HP1α's SUMOylation state. Hence, reducing the predominant SENP7L population in GILM2 cells reverts the EMT response (Fig. S6*F*) and significantly reduces the invasive, tumorigenic, and metastatic potential of these BCa cells (Fig. 6 *C–F*). Collectively the results support that induction of SENP7L favors BCa cell survival and EMT properties as outlined in Fig. 7. The present findings warrant the need to investigate the prometastatic/invasive properties of SENP7 further in whole animals.

Materials and Methods

All cell lines were grown and maintained as described in *SI Materials and Methods*. University of Texas M. D. Anderson Cancer Center guidelines were followed for the housing, caring, and use of mice. Detailed protocols for all experiments are presented in *SI Materials and Methods*.

ACKNOWLEDGMENTS. SENP7 and HP1α interaction was originally identified by Fei Gao. We thank Runsheng Wang for his great contribution to the manuscript. This project is supported in part by National Institutes of Health Grant RO1 CA239520 (to E.T.H.Y.). E.T.H.Y. is the McNair Scholar of the Texas Heart Institute.

1. Bawa-Khalfe T, Cheng J, Lin SH, Ittmann MM, Yeh ET (2010) SENP1 induces prostatic intraepithelial neoplasia through multiple mechanisms. *J Biol Chem* 285:25859–25866.
2. Bawa-Khalfe T, Yeh ET (2010) SUMO losing balance: SUMO proteases disrupt SUMO homeostasis to facilitate cancer development and progression. *Genes Cancer* 1: 748–752.
3. Yeh ET, Gong L, Kamitani T (2000) Ubiquitin-like proteins: New wines in new bottles. *Gene* 248:1–14.
4. Alegre KO, Reverter D (2011) Swapping small ubiquitin-like modifier (SUMO) isoform specificity of SUMO proteases SENP6 and SENP7. *J Biol Chem* 286:36142–36151.
5. Lima CD, Reverter D (2008) Structure of the human SENP7 catalytic domain and poly-SUMO deconjugation activities for SENP6 and SENP7. *J Biol Chem* 283:32045–32055.
6. Maison C, et al. (2012) The SUMO protease SENP7 is a critical component to ensure HP1 enrichment at pericentric heterochromatin. *Nat Struct Mol Biol* 19:458–460.
7. Kang X, et al. (2010) SUMO-specific protease 2 is essential for suppression of polycomb group protein-mediated gene silencing during embryonic development. *Mol Cell* 38:191–201.
8. Maison C, et al. (2011) SUMOylation promotes de novo targeting of HP1α to pericentric heterochromatin. *Nat Genet* 43:220–227.
9. Shin JA, et al. (2005) SUMO modification is involved in the maintenance of heterochromatin stability in fission yeast. *Mol Cell* 19:817–828.
10. Norwood LE, et al. (2006) A requirement for dimerization of HP1Hsalpha in suppression of breast cancer invasion. *J Biol Chem* 281:18668–18676.
11. De Koning L, et al. (2009) Heterochromatin protein 1alpha: A hallmark of cell proliferation relevant to clinical oncology. *EMBO Mol Med* 1:178–191.
12. Kirschmann DA, et al. (2000) Down-regulation of HP1Hsalpha expression is associated with the metastatic phenotype in breast cancer. *Cancer Res* 60:3359–3363.
13. Kalluri R, Weinberg RA (2009) The basics of epithelial-mesenchymal transition. *J Clin Invest* 119:1420–1428.
14. Narita M, et al. (2003) Rb-mediated heterochromatin formation and silencing of E2F target genes during cellular senescence. *Cell* 113:703–716.
15. Panteleeva I, et al. (2007) HP1alpha guides neuronal fate by timing E2F-targeted genes silencing during terminal differentiation. *EMBO J* 26:3616–3628.
16. Rastogi S, et al. (2006) Prohibitin facilitates cellular senescence by recruiting specific corepressors to inhibit E2F target genes. *Mol Cell Biol* 26:4161–4171.
17. Hu J, et al. (2011) Downregulation of transcription factor Oct4 induces an epithelial-to-mesenchymal transition via enhancement of Ca2+ influx in breast cancer cells. *Biochem Biophys Res Commun* 411:786–791.
18. Guan F, Handa K, Hakomori SI (2009) Specific glycosphingolipids mediate epithelial-to-mesenchymal transition of human and mouse epithelial cell lines. *Proc Natl Acad Sci USA* 106:7461–7466.
19. Nielsen SJ, et al. (2001) Rb targets histone H3 methylation and HP1 to promoters. *Nature* 412:561–565.
20. Maehara K, et al. (2005) Reduction of total E2F/DP activity induces senescence-like cell cycle arrest in cancer cells lacking functional pRB and p53. *J Cell Biol* 168:553–560.
21. Ansieau S, et al. (2008) Induction of EMT by twist proteins as a collateral effect of tumor-promoting inactivation of premature senescence. *Cancer Cell* 14:79–89.
22. Liu Y, El-Naggar S, Darling DS, Higashi Y, Dean DC (2008) Zeb1 links epithelial-mesenchymal transition and cellular senescence. *Development* 135:579–588.
23. Kokura K, Sun L, Bedford MT, Fang J (2010) Methyl-H3K9-binding protein MPP8 mediates E-cadherin gene silencing and promotes tumour cell motility and invasion. *EMBO J* 29:3673–3687.
24. Sánchez-Tilló E, et al. (2010) ZEB1 represses E-cadherin and induces an EMT by recruiting the SWI/SNF chromatin-remodeling protein BRG1. *Oncogene* 29:3490–3500.